Comparison of measurements and model calculations of stratospheric bromine monoxide

B.-M. Sinnhuber,[1,10] D. W. Arlander,[2] H. Bovensmann,[3] J. P. Burrows,[3]
M. P. Chipperfield,[1] C.-F. Enell,[4] U. Frieß,[5] F. Hendrick,[6] P. V. Johnston,[7] R. L. Jones,[8]
K. Kreher,[7] N. Mohamed-Tahrin,[8] R. Müller,[3] K. Pfeilsticker,[5] U. Platt,[5]
J.-P. Pommereau,[9] I. Pundt,[5,9] A. Richter,[3] A. M. South,[8] K. K. Tørnkvist,[2]
M. Van Roozendael,[6] T. Wagner,[5] and F. Wittrock[3]

[1] Ground-based zenith sky UV−visible measurements of stratospheric bromine monoxide (BrO) slant column densities are compared with simulations from the SLIMCAT three-dimensional chemical transport model. The observations have been obtained from a network of 11 sites, covering high and midlatitudes of both hemispheres. This data set gives for the first time a near-global picture of the distribution of stratospheric BrO from ground-based observations and is used to test our current understanding of stratospheric bromine chemistry. In order to allow a direct comparison between observations and model calculations, a radiative transfer model has been coupled to the chemical model to calculate simulated slant column densities. The model reproduces the observations in general very well. The absolute amount of the BrO slant columns is consistent with a total stratospheric bromine loading of 20 ± 4 ppt for the period 1998–2000, in agreement with previous estimates. The seasonal and latitudinal variations of BrO are well reproduced by the model. In particular, the good agreement between the observed and modeled diurnal variation provides strong evidence that the BrO-related bromine chemistry is correctly modeled. A discrepancy between observed and modeled BrO at high latitudes during events of chlorine activation can be resolved by increasing the rate constant for the reaction $BrO + ClO \rightarrow BrCl + O_2$ to the upper limit of current recommendations. However, other possible causes of the discrepancy at high latitudes cannot be ruled out.   *INDEX TERMS:* 0340 Atmospheric Composition and Structure: Middle atmosphere—composition and chemistry; 0394 Atmospheric Composition and Structure: Instruments and techniques

Citation: Sinnhuber, B.-M., et al., Comparison of measurements and model calculations of stratospheric bromine monoxide, *J. Geophys. Res.*, *107*(D19), 4398, doi:10.1029/2001JD000940, 2002.

1. Introduction

[2] Bromine compounds are believed to play an important role in the destruction of stratospheric ozone, both at high and midlatitudes [e.g., *World Meteorological Organization (WMO)*, 1999 and references therein; *Daniel et al.*,

1999]. Model calculations show that bromine reactions may contribute more than 50% to the seasonal Arctic ozone depletion [*Chipperfield and Pyle*, 1998]. Also in the midlatitude lower stratosphere, catalytic bromine reactions account for a large fraction of the halogen induced ozone loss [*Wennberg et al.*, 1994].

[3] The origin of atmospheric bromine is both natural and anthropogenic. However, due to the emission of anthropogenic compounds there has been a large increase of the atmospheric bromine loading from about 10 parts per 10^{12} by volume (ppt) in the 1970s to about 20 ppt in 2000 [*Fraser et al.*, 1999; *Sturges et al.*, 2001]. The major sources of stratospheric bromine are methyl bromide (CH_3Br), halons, especially Halon-1211 ($CBrClF_2$), Halon-1301 ($CBrF_3$) and Halon-2402 ($CBrF_2CBrF_2$), as well as bromochloromethane (CH_2BrCl) and dibromomethane (CH_2Br_2) [*Fraser et al*, 1999; *WMO*, 1999, chapter 1], with methyl bromide being the most abundant bromine source gas, accounting for about 50% of the current atmospheric sources. In addition it has recently been proposed [e.g.,

---

[1]School of the Environment, University of Leeds, UK.
[2]Norwegian Institute for Air Research, Kjeller, Norway.
[3]Institute of Environmental Physics, University of Bremen, Germany.
[4]Swedish Institute of Space Physics, Kiruna, Sweden.
[5]Institute of Environmental Physics, University of Heidelberg, Germany.
[6]Belgian Institute for Space Aeronomy, Brussels, Belgium.
[7]National Institute of Water and Atmospheric Research, Lauder, New Zealand.
[8]Centre for Atmospheric Science, University of Cambridge, UK.
[9]Service d'Aéronomie, Verrières-le-Buisson, France.
[10]Now at Institute of Environmental Physics, University of Bremen, Germany.

Ko et al., 1997; Dvortsov et al., 1999; Schauffler et al., 1999; Pfeilsticker et al., 2000; Sturges et al., 2000] that there could be a significant contribution of short-lived organic (e.g., bromoform, $CHBr_3$) and inorganic tropospheric sources to the total bromine loading of the stratosphere. This would then lead to a higher total bromine loading of the stratosphere than deduced from measurements of the organic source gases alone.

[4] Despite its importance for stratospheric ozone chemistry, there are few measurements of inorganic bromine compounds in the stratosphere. Except for BrO, there exist no measurements of the major inorganic bromine species; in particular $BrONO_2$ and BrCl have never been observed in the stratosphere. For HOBr there exist only measurements of upper limits [Johnson et al., 1995].

[5] Stratospheric BrO has been measured by ground-based zenith sky UV–visible spectroscopy [Carroll et al., 1989; Arpag et al., 1994; Fish et al., 1995; Aliwell et al., 1997; Eisinger et al., 1997; Kreher et al., 1997; Otten et al., 1998; Frieß et al., 1999; Richter et al., 1999], balloon-borne UV–visible spectroscopy [e.g., Harder et al., 1998; Pundt et al., 1999b; Fitzenberger et al., 2000; Harder et al., 2000] and in-situ resonance fluorescence spectroscopy both from aircraft [e.g., Brune et al., 1988, 1989; Toohey et al., 1990; Avallone et al., 1995] and balloon [McKinney et al., 1997].

[6] The recent balloon borne UV–visible measurements of BrO [e.g., Harder et al., 1998; Pundt et al., 1999b; Harder et al., 2000] showed relatively good agreement with model calculations. This is in contrast to in-situ BrO observations from the ER-2 aircraft [Avallone et al., 1995], which indicated a BrO/Br_y ratio in the lower stratosphere of about 40%, compared to about 60% calculated by photochemical models.

[7] Renard et al. [1998] showed evidence from balloon-borne spectroscopic measurements that OBrO could be present in significant amounts in the stratosphere and could even be a major nighttime bromine reservoir. However, the formation of significant amounts of OBrO in the stratosphere cannot be explained with our current understanding of the atmospheric bromine chemistry [Chipperfield et al., 1998]. Moreover, Erle et al. [2000] reported measurements of upper limits of OBrO which argue against OBrO being a significant nighttime bromine reservoir.

[8] Here we compare ground-based UV–visible measurements of BrO from a network of observing stations with calculations from the SLIMCAT global 3D chemical transport model (CTM) [Chipperfield, 1999]. The measurements have been performed from a network of sites ranging from the Arctic, over northern and southern hemisphere midlatitudes to Antarctica, most of them part of the Network for the Detection of Stratospheric Change (NDSC). We focus on a period of two and a half years from January 1998 until June 2000, allowing us to investigate the seasonal, and to some extent the inter-annual, variation of BrO. Previous studies [e.g., Fish et al., 1995, 1997; Frieß et al., 1999] have been limited to short periods and individual locations.

[9] The interpretation of the zenith sky UV–visible measurements is complicated, as the primary quantity measured is the BrO slant column density (SCD) along the slant path traversed by the scattered sunlight. This is even further complicated by the fact that BrO can vary strongly with solar zenith angle (SZA) along the slant path.

To allow a direct comparison between observed and modeled BrO, we simulate the measurement geometry by coupling a radiative transfer model to the chemical model to calculate simulated BrO slant column densities.

[10] In section 2 we briefly review our current understanding of stratospheric bromine chemistry. Sections 3 and 4 then describe the measurements and the model, respectively. The comparison between measurements and model is presented in section 5. In section 6 we present some sensitivity studies to investigate the impact of different processes on the modeled slant column densities. A discussion of the results and our conclusions are given in sections 7 and 8.

2. Stratospheric Bromine Chemistry

[11] Unlike chlorine, a large fraction of the lower stratospheric inorganic bromine during daytime is present in reactive form as BrO. The following reactions
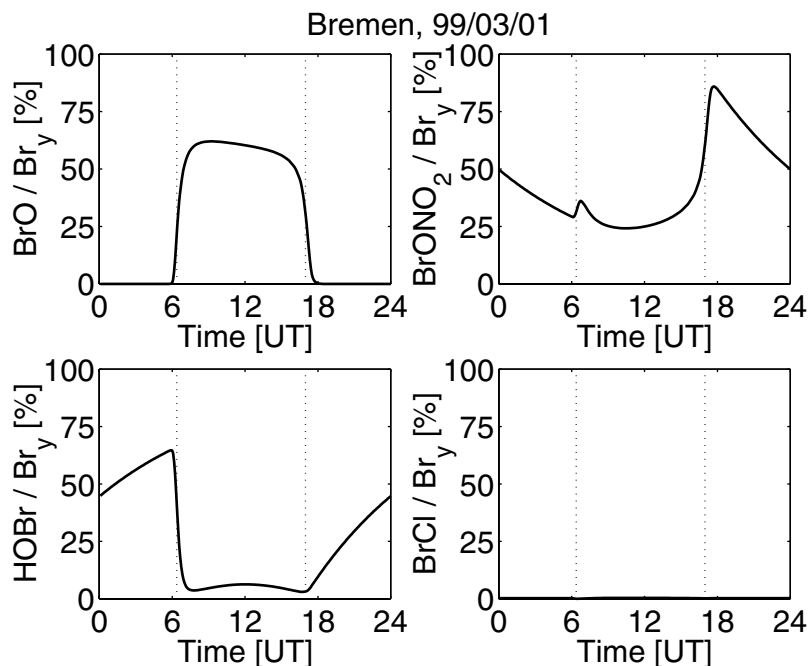
$$BrO + NO_2 + M \rightarrow BrONO_2 + M, \qquad (1)$$

$$BrO + HO_2 \rightarrow HOBr + O_2, \qquad (2)$$

and

$$BrO + ClO \rightarrow BrCl + O_2 \qquad (3a)$$

$$\rightarrow Br + ClOO \qquad (3b)$$

$$\rightarrow Br + OClO \qquad (3c)$$

convert BrO into the main bromine reservoirs bromine nitrate ($BrONO_2$), HOBr and BrCl. During daytime BrO is quickly released from the reservoir species by photolysis or by the reaction of HOBr with $O(^3P)$. Recent laboratory measurements by Soller et al. [2001] indicate that the reaction $BrONO_2 + O(^3P)$ could be an important source of BrO (see section 6.4). Bromine nitrate is believed to be the major bromine reservoir species, accounting for roughly half of the inorganic bromine in the lower stratosphere, except for periods of high chlorine activation. Despite its important role in stratospheric bromine chemistry, bromine nitrate has never been measured in the stratosphere.

[12] Bromine nitrate can be converted heterogeneously by hydrolysis on sulfate aerosols into HOBr [Hanson and Ravishankara, 1995; Hanson et al., 1996]:

$$BrONO_2 + H_2O(aq) \rightarrow HOBr + HNO_3. \qquad (4)$$

As a result of the hydrolysis of $BrONO_2$, we expect HOBr to be a major bromine reservoir before sunrise in the lower stratosphere. The hydrolysis of $BrONO_2$ is also of general importance, as it influences the HO_x and NO_x abundances, which has significant direct and indirect effects on the lower stratospheric ozone depletion [Hanson et al., 1996; Lary et al., 1996]. Lary et al. [1996] showed that reaction (4) is consistent with the rapid increase of HO_x at sunrise due to the photolysis of HOBr, as observed by Salawitch et al. [1994]. Observational evidence for the importance of reaction (4) on cold stratospheric aerosols for halogen activation has been presented by Erle et al. [1998]. Slusser

Figure 1. Diurnal cycle of the relative contribution of the most abundant bromine species BrO, BrONO$_2$, HBr and BrCl in the lower stratosphere (480 K isentropic level, 58 hPa), calculated by the photochemical model described in the text. This example for Bremen (53°N) for 1 March 1999 shows the typical bromine partitioning at midlatitudes.

et al. [1997] presented observational evidence that reaction (4) had a significant impact in reducing stratospheric NO$_x$ in the presence of Pinatubo aerosols.

[13] At higher altitudes between about 25–35 km, HOBr becomes less important. Here inorganic bromine is predominantly partitioned between BrO and BrONO$_2$.

[14] As an example, Figure 1 shows the modeled diurnal cycle of bromine partitioning in the lower stratosphere, calculated by the model described in section 4 below. This example for Bremen (53°N) for 1 March 1999 shows the typical behavior at midlatitudes in the lower stratosphere: BrO is about 60% of the available inorganic bromine during daytime, with bromine nitrate the most important bromine reservoir. Bromine nitrate is heterogeneously converted into HOBr during nighttime (reaction 4), which is then the major bromine reservoir at sunrise.
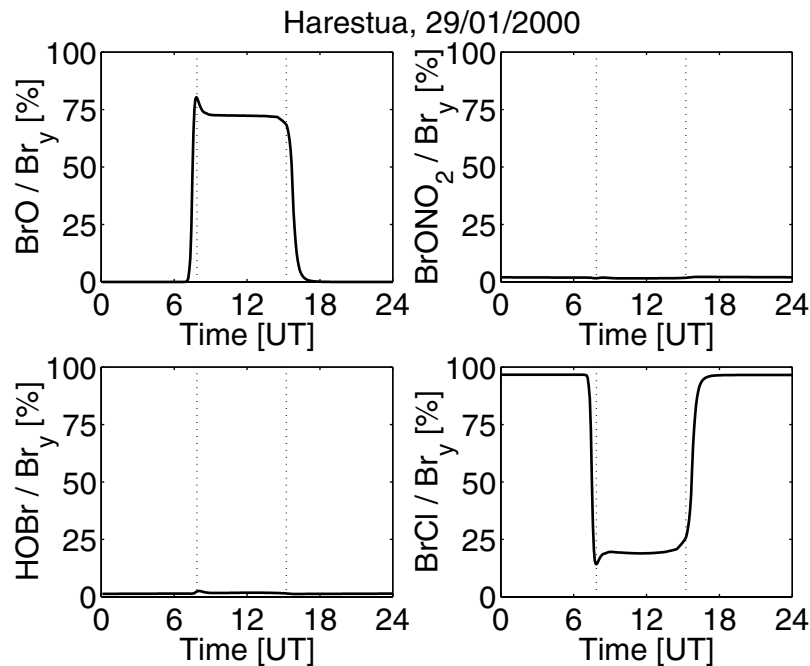
[15] In contrast, Figure 2 shows the situation for high chlorine activation for Harestua (60°N) for 29 January 2000. The concentrations of BrONO$_2$ and HOBr are very low and the inorganic bromine is almost exclusively partitioned between BrO and BrCl.

3. Measurements

[16] The measurements reported in this study were obtained by zenith sky UV–visible spectroscopy, performed at 11 stations. The measurement sites range from northern high latitudes (Ny-Ålesund, Andøya, Kiruna), over northern midlatitudes (Harestua, Bremen, Cambridge, Observatoire de Haute-Provence, OHP, Huelva), southern midlatitudes (Lauder) to southern high latitudes (Neumayer, Arrival Heights), see Table 1.

[17] This work relies on a network of UV–visible spectrometers set up to observe the zenith scattered sunlight in the spectral region between 346 and 359 nm, where BrO can be measured by the method of differential optical absorption spectroscopy (DOAS) [e.g., *Platt*, 1994]. The instruments share the same general design, based on the use of thermally stabilized grating spectrometers equipped with low-noise cooled array detectors, optimized for the detection of weak atmospheric absorbers in the UV–visible region. All spectrometers are largely oversampled with resolutions in the range from 0.6 to 0.9 nm, which provide a good compromise between resolution and light throughput resulting in optimal sensitivity to the vibrational absorption structures of BrO.

[18] At all sites the DOAS analysis for BrO is performed according to the precise guidelines developed and extensively described by *Aliwell et al.* [2002], based on the results of the BrO intercomparison campaign held at Observatoire de Haute Provence in June 1996. These guidelines include recommendations on the wavelength range to be used (346–359 nm) as well as the number and nature of absorption cross-sections to be included in the DOAS analysis. Note that all groups involved in the present study also took part in this former exercise, which resulted in the cross-validation of the different analysis software tools used at the various institutes and, in general, significantly contributed to the improvement of the consistency of the BrO data set used in the present work. The precision of the BrO observations reported here is about 15% (1σ), as derived from the spectral fits. The absolute accuracy is limited by the uncertainty in the temperature-dependent BrO absorption cross-sections as well as by more subtle spectral

Figure 2. As Figure 1 but for Harestua (60°N) for 29 January 2000 (480 K isentropic level, 40 hPa). This example shows the bromine partitioning for a situation of high chlorine activation.

interference effects known to produce offsets in the data retrieval depending on the analysis settings adopted [*Aliwell et al.*, 2002]. The uncertainty of the BrO cross-sections is about ±10% at 223 K, but could be larger at cold temperatures [e.g., *Harder et al.*, 2000]. As a result of the temperature dependence of the BrO cross-sections, it is likely that the retrievals overestimate the true BrO slant columns by up to 20% at low polar temperatures. We thus estimate the overall accuracy of the measurements to be better than 23% for all cases except cold polar conditions, and better than 30% for cold polar conditions (1σ).

[19] This study compares observations and model simulations of the difference in BrO slant column between 90° and 80° SZA. Differential slant columns are the natural product of the zenith sky DOAS observations and have generally been reported as such in previous studies on BrO because of the significant uncertainties that would affect the conversion to vertical column amounts without accounting properly for the strong diurnal change of BrO [*Fish et al.*, 1995]. The choice of the 90–80° SZA range was done primarily to optimize the signal-to-noise ratio of the differential BrO absorption. However, this choice also presents the advantage of maximizing the sensitivity of the observation to the stratospheric part of the BrO profile, due to the strong geometrical enhancement of the optical path in the stratosphere at twilight [e.g., *Solomon et al.*, 1987] and the comparatively small variation of the tropospheric air mass factor.

[20] We focus here on a period of two and a half years from January 1998 to June 2000. This period was chosen to have maximum overlap between the BrO time series from

Table 1. Geographic Locations of the BrO Measurement Sites

Station	Latitude	Longitude	Institution	Reference
		Arctic		
Ny-Ålesund, Spitsbergen	79°N	12°E	U. Bremen	*Eisinger et al.* [1997]
Andøya, Norway	69°N	16°E	NILU	*Tørnkvist et al.* [2002]
Kiruna, Sweden	68°N	21°E	U. Heidelberg/IRF Kiruna	*Otten et al.* [1998]
		Northern Midlatitude		
Harestua, Norway	60°N	10°E	IASB-BIRA	*Van Roozendael et al.* [1999a]
Bremen, Germany	53°N	9°E	U. Bremen	*Eisinger et al.* [1997]
Cambridge, United Kingdom	52°N	0°E	U. Cambridge	*Fish et al.* [1995]
Observatoire de Haute-Provence, OHP, France	44°N	6°E	IASB-BIRA	*Van Roozendael et al.* [1999a]
Huelva, Spain	37°N	7°W	U. Cambridge	*South et al.* [1999]
		Southern Midlatitude		
Lauder, New Zealand	45°S	167°E	NIWA	*Kreher et al.* [1997]
		Antarctic		
Neumayer Station, Antarctica	70°S	8°W	U. Heidelberg	*Frieß et al.* [2001]
Arrival Heights, Antarctica	78°S	167°E	NIWA	*Kreher et al.* [1997]

the different stations. In addition, we included winter and spring 2000 to allow a comparison between the relatively warm stratospheric conditions during the Arctic winters 1997/1998 and 1998/1999 and the cold stratospheric conditions during winter 1999/2000.

4. Model

[21] The model used in this study is the SLIMCAT global 3D chemical transport model (CTM), described in detail by *Chipperfield* [1999]. The model is forced by temperature and horizontal wind fields from UKMO analyses [*Swinbank and O'Neill*, 1994]. It was initialized in October 1991 from a 2D (latitude-height) model and then integrated at $5° \times 7.5°$ horizontal resolution. The model as used in this study has 12 isentropic levels, ranging from 335 to 2700 K, corresponding to an altitude range of approximately 10 to 55 km. Vertical transport across isentropic levels is calculated from interactively computed diabatic heating rates. At the lower boundary mixing ratios from 2D model results are prescribed to account for trace gas fluxes into the model domain from below. Liquid aerosol is calculated from the H_2SO_4 loading, specified month-by-month from detailed two-dimensional (latitude-height) time-dependent calculations [*Bekki and Pyle*, 1994] and advected as a passive tracer by the CTM.

4.1. Chemistry

[22] The model calculations shown here used photochemical reaction rate constants and photolysis cross-sections from the JPL 1997 reaction rate recommendations [*DeMore et al.*, 1997] with a few exceptions: Reaction rate constants for $NO_2 + OH \rightarrow HNO_3$ and $HNO_3 + OH \rightarrow NO_3 + H_2O$ were taken from *Brown et al.* [1999a] and *Brown et al.* [1999b], respectively. These rates have a significant impact on the NO_x/NO_y ratio and thus on the BrO concentrations. We find that the use of these updated reaction rates decreases the BrO concentrations by approximately 10% in the midlatitude lower stratosphere, compared to JPL 1997 reaction rates. The decrease in BrO is smaller than the increase in $BrONO_2$ (approximately 20%), since part of the increase in $BrONO_2$ is compensated by a decrease in HOBr. Another exception from JPL 1997 is that we use the HOBr photolysis cross-sections from *Ingham et al.* [1998], which clearly shows a third absorption band centered at 457 nm, resulting in a faster HOBr photolysis compared to JPL 1997 recommendations. All changes from JPL 1997 kinetics described so far are now also included in the recent JPL 2000 reaction rate recommendations [*Sander et al.*, 2000]. In addition, the branching ratio of the $BrONO_2$ photolysis has recently been measured by *Harwood et al.* [1998]. Their result shows a quantum yield of close to unity for the production of NO_3 in the relevant wavelength range. This is in clear contrast to the JPL 1997 recommendations. In the present study we thus assume that the production of $Br + NO_3$ is the only channel.

[23] The model calculations assume a total bromine loading of 20 ppt, which is in agreement with observations of organic bromine compounds of 18 ppt for 1994 and 20 ppt for 1996 by *Wamsley et al.* [1998] and *Schauffler et al.* [1999], respectively, and an inferred total bromine loading from balloon borne BrO measurements of 20 ppt for 1996 and 21.5 ppt for 1998/1999 by *Harder et al.* [2000] and *Pfeilsticker et al.* [2000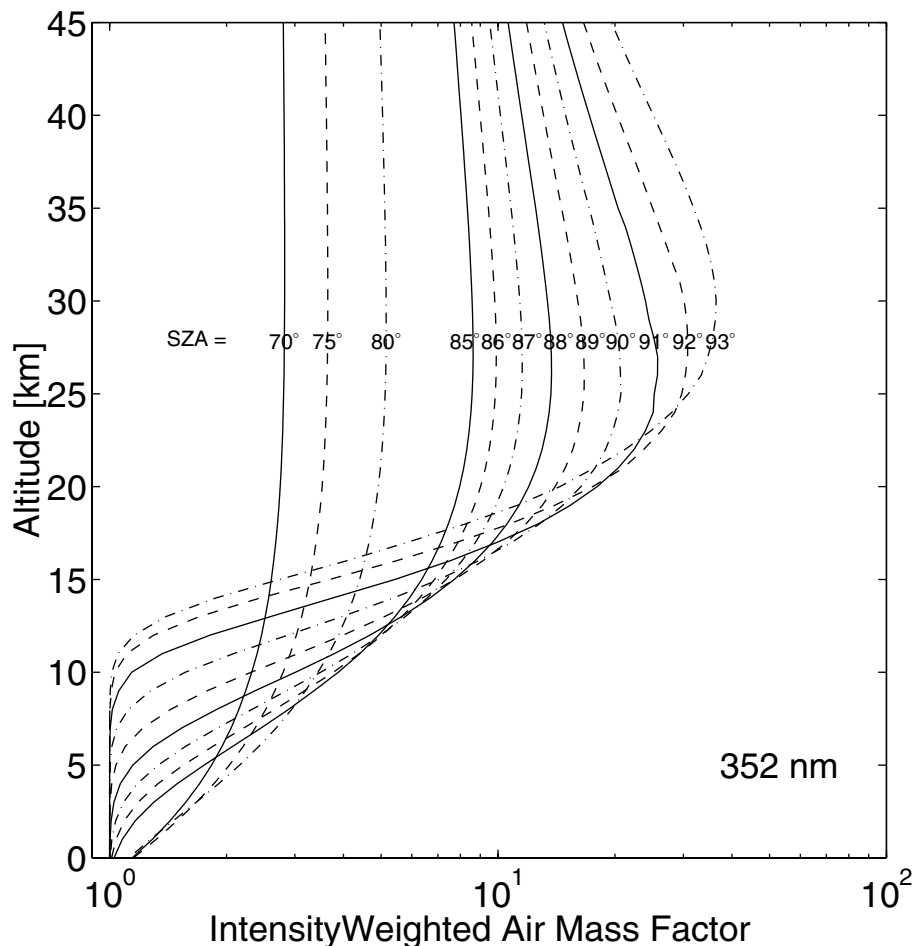], respectively. The only bromine source gas in the model is methyl bromide, CH_3Br, which is scaled to produce a realistic total organic bromine loading. This approach leads to a reasonable approximation of the total inorganic bromine (Br_y) profile, since (a) the rate of release of bromine is similar for most of the different organic source gases [*Wamsley et al.*, 1998, Table 4] and (b) CH_3Br is by far the most important bromine source gas anyway, accounting for more than 50% of the organic bromine loading. A more detailed estimation shows, that the use of CH_3Br as the only bromine source gas will underestimate the inorganic bromine loading in the lowermost stratosphere by less than about 1 ppt (or about 25%), based on the empirical correlation of the different bromine source gases with $CFCl_3$ (CFC-11) from *Wamsley et al.* [1998]. *Pundt et al.* [1999b] found good agreement between vertical profiles of Br_y derived empirically from in-situ measurements of CFC-11 and modeled Br_y profiles from the SLIMCAT CTM for Arctic and midlatitude conditions. More fundamental is probably the neglection in the model of any short-lived organic and inorganic bromine sources.

[24] The global output from the 3D CTM is saved only every second day at 12UT. The diurnal cycle of BrO at the stations is then calculated by a 1D column model (stacked box model) with identical chemistry as in the 3D CTM, initialized with the 3D model.

4.2. Calculation of Slant Columns

[25] To calculate BrO slant column densities from the modeled BrO, we have coupled a radiative transfer model to the chemistry model. The model takes into account single scattering by the so-called intensity weighting approach, as described by *Solomon et al.* [1987]. The model uses full spherical geometry and explicitly takes into account the variation of BrO with SZA along the slant path. Comparisons with two other radiative transfer models showed good agreement (F. Hendrick, unpublished manuscript) [see also *Hendrick et al.*, 1999]. Figure 3 shows the intensity-weighted air mass factor, that is the effective path length for a given SZA averaged over all possible scattering heights according to their contribution to the total intensity received at the ground. The BrO slant column density is similarly obtained by averaging the integrals of the BrO number density along the slant paths for all possible scattering heights, weighted by the total intensity received. The calculations were performed for a wavelength of 352 nm—corresponding to the center of the BrO fit window of the measurements—with the Rayleigh scattering cross-section taken from *Bates* [1984]. Note that the air mass factor approaches unity in the troposphere for large SZA. This is because at large SZA most of the scattering takes place in the stratosphere and the underlying tropospheric levels are traversed vertically. This means that any BrO amount below about 13 km effectively decreases the BrO $90°-80°$ differential slant columns, as can be seen from Figure 3. A more detailed analysis shows that under typical midlatitude conditions the largest contribution to the $90°-80°$ DSCD comes from a layer $\sim$10 km thick centered at about 22 km altitude. At high latitudes under conditions of enhanced chlorine activation the largest contribution comes from slightly lower altitudes, centered at about 18 km altitude.

[26] The calculations include only Rayleigh scattering and do not take into account the effect of refraction. In

Figure 3. Intensity weighted air mass factors (see text) as a function of altitude for different solar zenith angles (SZA).

section 6.2 we investigate the effect of aerosol scattering on the calculated BrO slant column densities.
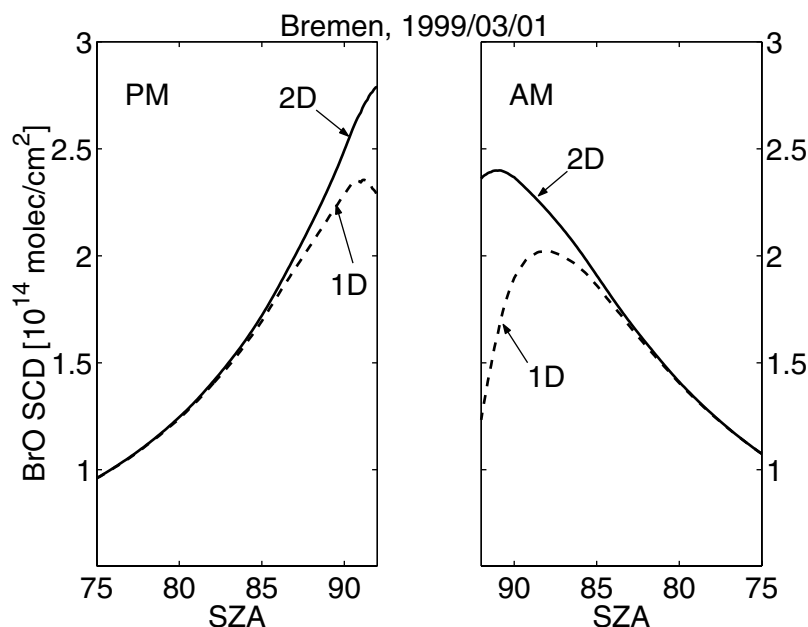
[27] An example of calculated BrO slant columns for 1 March 1999 for Bremen is shown in Figure 4. The treatment of the variation of BrO along the slant path has a very large impact on the slant column densities at large SZA, as BrO changes very rapidly around 90° SZA. This is shown in Figure 4 by comparing the calculated slant columns with the variation of BrO along the slant path taken into account (labeled "2D") and a calculation where BrO is constant along the slant path (labeled "1D"). It is essentially this variation of BrO along the slant path which makes a full multiple scattering calculation of BrO slant column densities difficult. In section 6.1 we show some comparisons of calculated BrO slant columns using this single scattering model with a novel multiple scattering calculation. However, since the multiple scattering calculations are very time consuming, we use the single scattering model for the comparison of measured and modeled BrO differential slant columns.

5. Comparison of Measured and Modeled Slant Columns

[28] Figure 5 shows the measured BrO 90–80° differential slant columns together with the model calculation for the different stations. The model reproduces the observa-

tions generally very well. The mean differences between measured and modeled BrO DSCD, calculated on a point-by-point basis, are shown in Table 2. For most of the stations measured DSCD are higher than modeled DSCD by about 10%. The scatter of the difference is about 20% for most of the stations. The differences, as well as the scatter, are generally about the same for sunrise (AM) and sunset (PM) observations. The fact that the mean discrepancies between measurements and model are similar for most of the stations, in particular for stations that are close to each other e.g., Kiruna and Andøya, demonstrates the good internal consistency of the observational network.

[29] However, two stations clearly stand out: For Ny-Ålesund (79°N) and Neumayer (70°S) the measurements are much lower than the model with a large scatter in the differences. As both stations are frequently located at the edge of the sea ice, it is likely that at least part of the discrepancy and scatter results from enhanced tropospheric boundary layer BrO events. Such events, which are observed both over the Arctic and Antarctic in spring [e.g., *Kreher et al.*, 1997; *Richter et al.*, 1998; *Wagner and Platt*, 1998; *Wagner et al.*, 2001], are likely related to processes when the sea ice breaks up in spring. *Kreher et al.* [1997] showed that these events lead to a decrease of the 90–80° BrO DSCD, basically due to the different air mass factors for tropospheric and stratospheric absorbers (see

Figure 4. Calculated BrO slant column densities for the example case for Bremen, 1 March 1999 shown in Figure 1. The line marked "2D" shows the result from the calculation including the variation of BrO with solar zenith angle along the slant path. This is compared to a calculation with constant BrO along the slant path (marked "1D").

Figure 3). For Arrival Heights, however, the differences between measurements and model are more in line with the other (midlatitude) stations. This is consistent with the fact, that events of enhanced tropospheric BrO are not often observed at this station.

[30] At Arrival Heights the difference between observed and modeled BrO DSCD is significantly larger during spring than during the rest of the year. During spring, the model overestimates the observations (for both, AM and PM) by about 20%. A similar discrepancy of about 20% can also be seen, for example, at Kiruna and Andøya in early March 2000 and at Harestua under the influence of polar vortex air masses. It is thus likely related to situations of enhanced chlorine activation, where BrCl becomes the main bromine reservoir. The temperature dependence of the BrO absorption cross-section is most likely to be of the opposite sense, with the cross-section likely being larger by about 12% at 195 K compared to 223 K. As this is not taken into account in the BrO retrievals in this study, it is likely that the difference under cold polar conditions is even larger.

[31] The seasonal and latitudinal variations of the observed BrO DSCD are generally well reproduced by the model. The seasonal and latitudinal variations are basically due to the combined effect of variations of the Br_y column due to transport and variations of the bromine partitioning due to chemistry. The Br_y column shows a seasonal variation similar to total ozone, with a maximum in late winter and spring and a minimum in late fall. The BrO/Br_y ratio on the other hand shows a seasonal cycle with a maximum in winter of about 70% and a minimum in summer of about 50% at midlatitudes, as it is driven mainly by the seasonal cycle of NO_2 in the lower stratosphere. While the day-to-day variability in the BrO column at a given location is largely a result of changes in the Br_y

column, the seasonal cycle of BrO is dominated by changes in bromine partitioning.

[32] For a number of cases there are events of enhanced BrO DSCD observed at midlatitudes, most clearly seen at Harestua and Bremen. These events are associated with the advection of polar vortex air masses and are, in many cases, also reproduced by the model.

[33] The model also reproduces the diurnal cycle generally very well, with PM BrO DSCD generally larger than AM DSCD. This diurnal cycle is most clearly seen at the midlatitude sites of OHP and Lauder (44°N and 45°S, respectively), with a maximum in winter and a minimum in summer. At higher latitudes the AM/PM variation is much smaller and also well reproduced by the model. At polar latitudes, during events of large chlorine activation in spring, the model shows a reversed AM/PM ratio, with BrO DSCD higher at AM than PM, in agreement with the observations [see also *Tørnkvist et al.*, 2002].

[34] To allow a better comparison of the diurnal variation, Figure 6 shows the difference of the PM-AM BrO differential slant columns for OHP and Lauder. The diurnal cycle is most clearly seen at these stations, thus providing a good test for the model's chemistry. The error bars in Figure 6 represent monthly averages and their standard deviation. In the case of the measurements the errors thus represent the precision of the measurements plus the atmospheric variability, while in the case of the model they represent only the atmospheric variability. For both stations the agreement between the observed and modeled diurnal variation is very good. The model agrees well with the observations within their standard deviation. Both the absolute amount, as well as the seasonal variation of the AM/PM variation are well reproduced. The AM/PM variation in the model is not influenced by any dynamical or radiative transfer effects,

but only by the diurnal cycle of the chemistry. This comparison thus provides a critical test for the model's stratospheric bromine chemistry. Note that the modeled AM/PM variation changed between 1998 and 1999/2000, being in better agreement with the observations at OHP during the latter years. It is caused by a decrease in NO_y in the model during this period, possibly as a result of changes in transport, linked to changes in the analyzed winds used to force the model.

[35] Although the measurements reported here cover a wide range of latitudes over both hemispheres, measurements of BrO in the tropics are notably missing. They would be needed to achieve a truly "global" picture of the stratospheric bromine chemistry. In Figure 7 we show the modeled BrO DSCD for a tropical site. The calculation has been performed for Kaashidhoo, Maldives (5°N, 73°E), where some of us (Richter and coworkers) performed BrO zenith sky measurements during February and March of 1999. Due to technical problems experienced during the campaign, BrO slant columns are still under evaluation. It is planned to continue UV–visible zenith sky measurements at Kaashidhoo in the near future. In addition, another group (Johnston and coworkers) started BrO zenith sky measurements at Hawaii (20°N) in December 1999.

6. Sensitivity Studies

[36] To investigate the impact of different processes on the calculation of the modeled BrO DSCD, a number of sensitivity calculations have been performed. In this section we discuss the impact of multiple scattering, aerosol scattering and a possible tropospheric BrO background on the modeled BrO DSCD. In addition we show the impact of uncertainties in the rate constants for the most important reactions.

6.1. Multiple Scattering

[37] To test the impact of the single scattering approximation on the calculated BrO slant column densities, we did comparisons with a full multiple scattering model which included the variation of BrO along the slant path [*Müller et al.*, 2002; *Rozanov et al.*, 2001]. Figure 8 shows the BrO slant column densities for single- and multiple scattering calculations. The single scattering approximation leads to an underestimation of the *absolute* BrO slant column density of about 2×10^{13} molecules/cm^2, about 10–15%. However, the impact on the *differential* slant column densities is much smaller. In fact, we found that the single scattering approximation can both underestimate or overestimate the BrO DSCD, depending on the BrO profile. In any case, the impact of the single scattering approximation on the differential slant column densities seems to be small. However, it may not be justified to ignore the effect of multiple scattering if one compares absolute slant column densities.

6.2. Aerosol Scattering

[38] Stratospheric aerosol can have an impact on the air mass factor [e.g., *Sarkissian et al.*, 1995], influencing the

measured BrO slant columns. To test the sensitivity of the calculated BrO slant columns due to aerosol scattering, we performed calculations with a standard aerosol extinction profile, representative for stratospheric background conditions (Figure 9). This assumed extinction profile is generally consistent with observations by the Polar Ozone and Aerosol Measurement III (POAM III) satellite instrument at 353.4 nm (Karl Hoppel, personal communication, 2000). The calculations assumed a Henyey-Greenstein phase function [e.g., *Liou*, 1992], using an asymmetry parameter of 0.7. Figure 10 shows the calculated impact of the assumed aerosol extinction profile on the BrO slant columns for a given day. For the case shown here, aerosol scattering leads to a reduction of the BrO slant column density of about 5% at 90° SZA. The calculations shown here also include a tropospheric aerosol extinction profile. However, it was found that tropospheric aerosols have only a small impact on the BrO slant column. We found that the relative impact of stratospheric aerosol scattering on the BrO DSCD for the same aerosol extinction profile is largest during winter and smallest during summer, which is essentially due to the different shape of the BrO profile. In any case we found that the inclusion of aerosol scattering for a stratospheric background aerosol profile leads to a reduction in the BrO DSCD of not more than about 10%. However, polar stratospheric clouds may have a substantial impact on the differential slant columns.

6.3. Tropospheric BrO Background

[39] To test the impact of a possible tropospheric BrO background on the calculated DSCD, a sensitivity calculation was performed with an assumed additional constant BrO mixing ratio of 1 ppt between the ground and the lowest stratospheric model level. This assumed tropospheric BrO background is similar to the inferred tropospheric BrO values of *Frieß et al.* [1999], *Pundt et al.* [1999a], *Van Roozendael et al.* [1999b], and the recently observed tropospheric BrO profile by *Fitzenberger et al.* [2000]. The result of this calculation is shown in Figure 11. The additional tropospheric BrO contribution leads to an increase in the absolute slant column densities of 1.7 to 2.9 $\times$ 10^{13} molecules/cm^2, with the smaller increase at larger SZA. Note that no diurnal variation of this assumed tropospheric BrO background has been considered. A constant tropospheric BrO contribution (or one which decreases with increasing SZA) will thus lead to a small decrease of the BrO slant column densities for 90–80°, as the absolute slant column contribution from the assumed tropospheric BrO background is higher for the reference at 80° than for 90°.

[40] Table 3 summarizes the results of the sensitivity calculations. The calculations in Table 3 have been performed for the midlatitude site of Bremen. Calculations for OHP for different seasons (for comparison with Figure 6) lead to basically the same results.
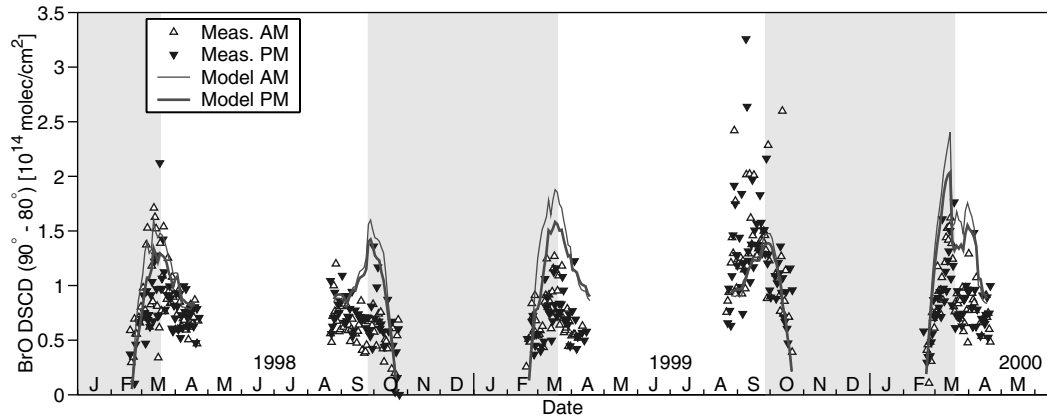
[41] As a result of these sensitivity studies, we see that differential slant columns are generally less affected than absolute slant columns. In particular multiple scattering and
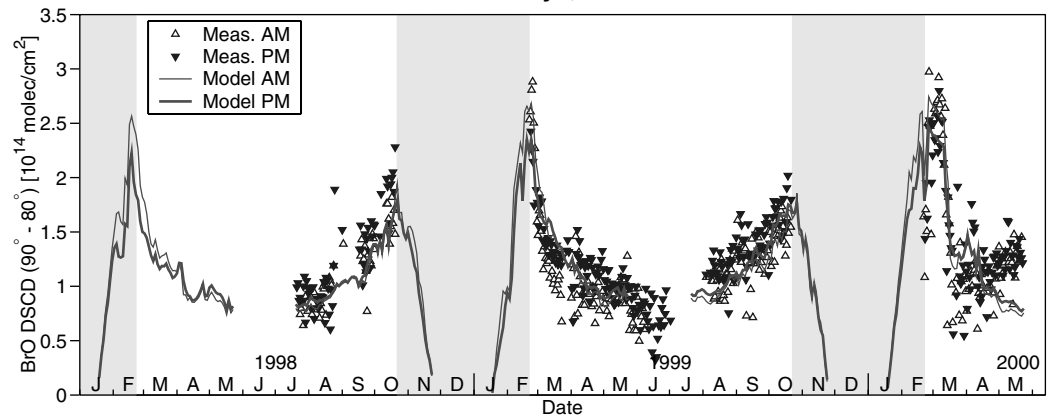

Figure 5. (opposite) Comparison of observed and modeled BrO differential slant column densities. Shown are differential slant columns between solar zenith angles of 90° and 80°. In some cases, when 80° were not reached at high latitudes, the local noon values were used as reference instead (shaded periods). For technical reasons DSCD for Bremen are given between 89° and 80°.
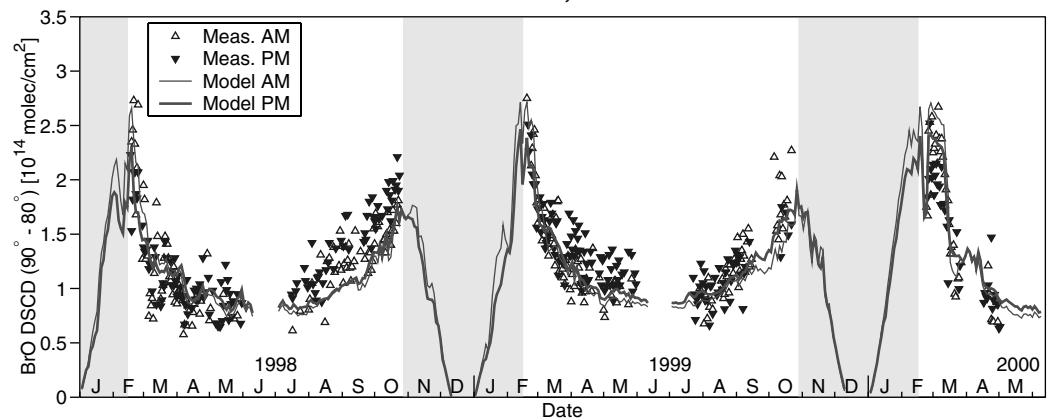
Ny-Alesund, 79° N

Andoya, 69° N
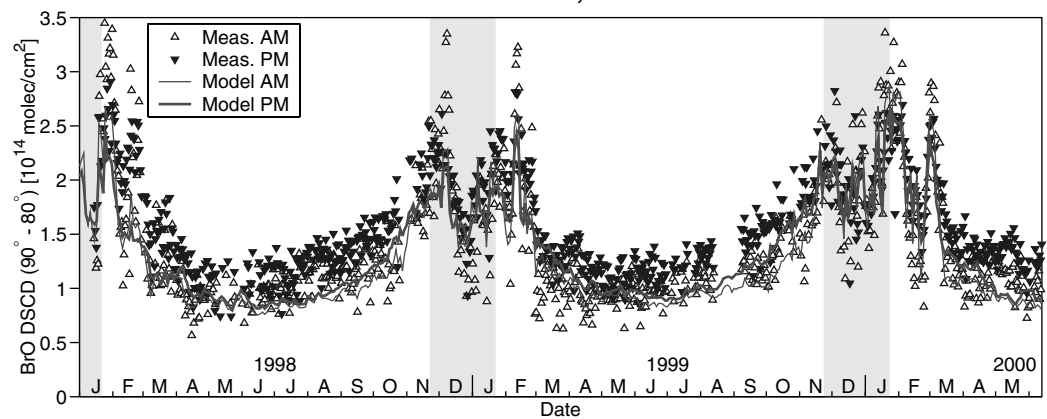

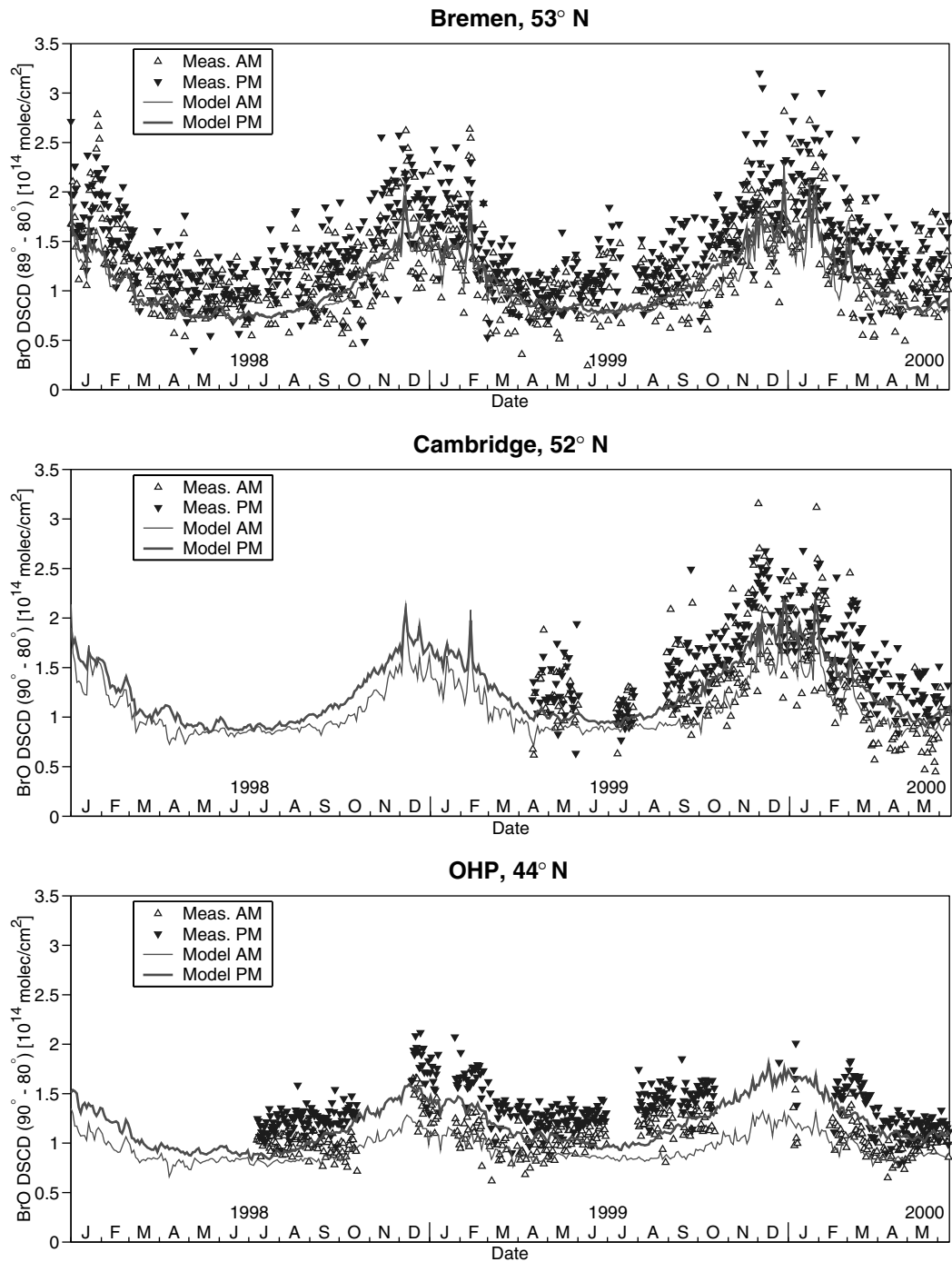**Kiruna, 68° N**
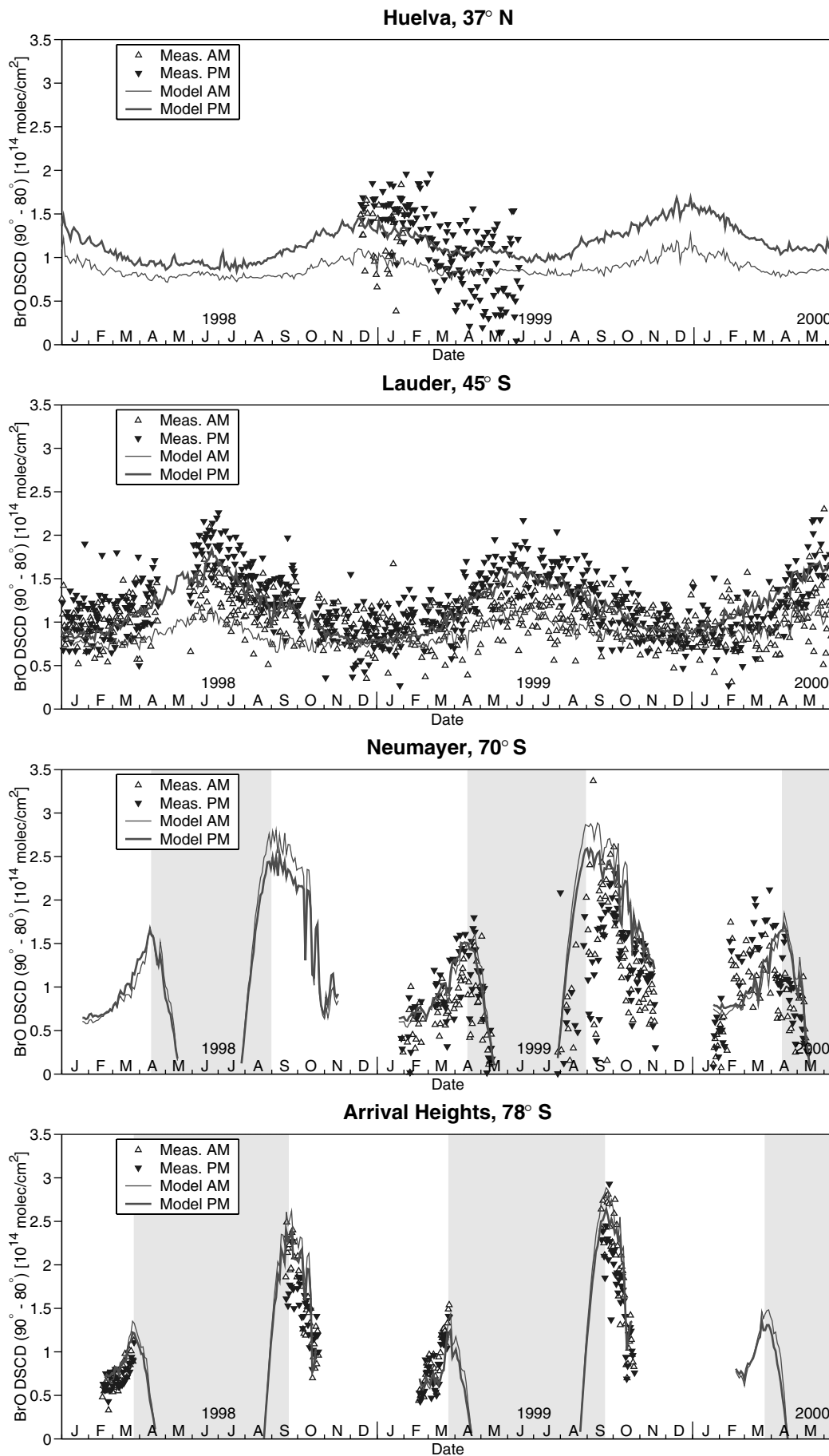

Harestua, 60° N

Figure 5. (continued)

Figure 5.   (continued)

Table 2. Mean Difference Between Observed and Modeled BrO DSCD at Different Stations

	Mean Difference (Measured − Modeled), in 10^{13} molecules/cm^2	
	AM	PM
Ny-Ålesund	−3.3 ± 4.6	−2.2 ± 4.2
Andøya	−0.1 ± 2.9	0.9 ± 2.4
Kiruna	0.4 ± 2.4	0.6 ± 2.4
Harestua	1.0 ± 2.7	2.3 ± 2.1
Bremen	1.9 ± 2.7	3.2 ± 3.0
Cambridge	2.2 ± 3.3	2.4 ± 2.5
OHP	1.7 ± 1.4	2.2 ± 1.6
Huelva[a]	2.8 ± 3.0	2.2 ± 2.2
Lauder	1.7 ± 2.3	0.7 ± 2.4
Neumayer	−3.8 ± 5.1	−2.9 ± 5.3
Arrival Heights[b]		
Spring	−3.6 ± 2.6	−4.2 ± 2.6
Rest of year	−0.1 ± 2.1	−0.2 ± 2.1

The uncertainties given are the standard deviations of the differences (1σ).

[a] For Huelva, only December 1998 and January 1999 were considered when both AM and PM observations were available.

[b] For Arrival Heights, "spring" (defined here as September 17 to October 17) and the rest of the year were considered separately. The differences for the whole period are $(-1.5 \pm 2.8) \times 10^{13}$ molecules/cm^2 for AM and $(-1.8 \pm 3.0) \times 10^{13}$ molecules/cm^2 for PM.

a tropospheric BrO contribution can have a significant impact on the absolute slant columns but appear to be only second order effects for the differential slant columns. The situation is a somewhat different for aerosol scattering, however, although we found that the impact of stratospheric background aerosol is likely to be small. It is interesting to note that basically all of the effects considered here lead to a decrease of the 90–80° BrO DSCD, compared to our standard calculations used in the comparisons in the previous section.
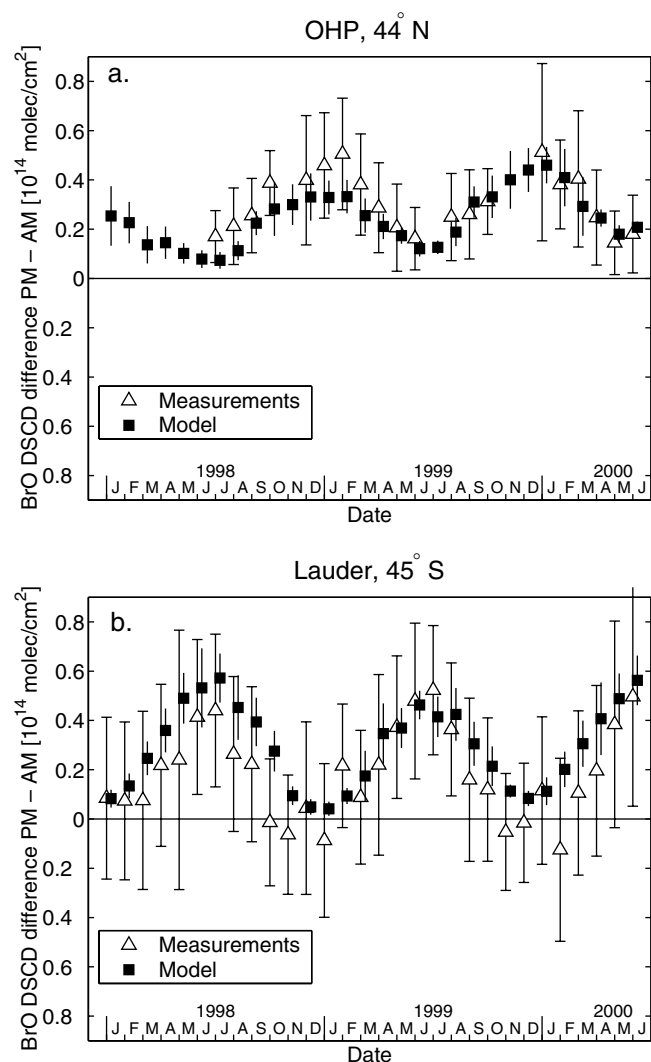
6.4. Uncertainties of Reaction Rates

[42] The BrO concentrations are, to a large extent, controlled by the NO_2 concentration through reaction (1). Reducing the reaction rate constant to the JPL 2000 lower limit increases the BrO DSCD at sunrise by about 5% and the BrO DSCD at sunset by about 17% for typical midlatitude conditions. Consequently, this increases the difference of the PM-AM BrO DSCD by more than 50%. (Note that the recommendation for the rate constant of reaction (1) did not change between JPL 1997 and JPL 2000, but the estimated uncertainty was decreased.)

[43] The new JPL 2000 reaction rate recommendations [*Sander et al.*, 2000] give a faster rate constant for the reaction $BrO + ClO \rightarrow BrCl + O_2$, resulting in an increase in BrCl and a decrease in BrO for situations of activated chlorine. However, the difference between the JPL 1997 and the JPL 2000 reaction rate constants is still well within the estimated uncertainty of the reaction rate constant [*Sander et al.*, 2000]. Increasing the rate constant to the JPL 2000 upper limit decreases the calculated BrO DSCD by about 15% for situations where BrCl is the major bromine reservoir.
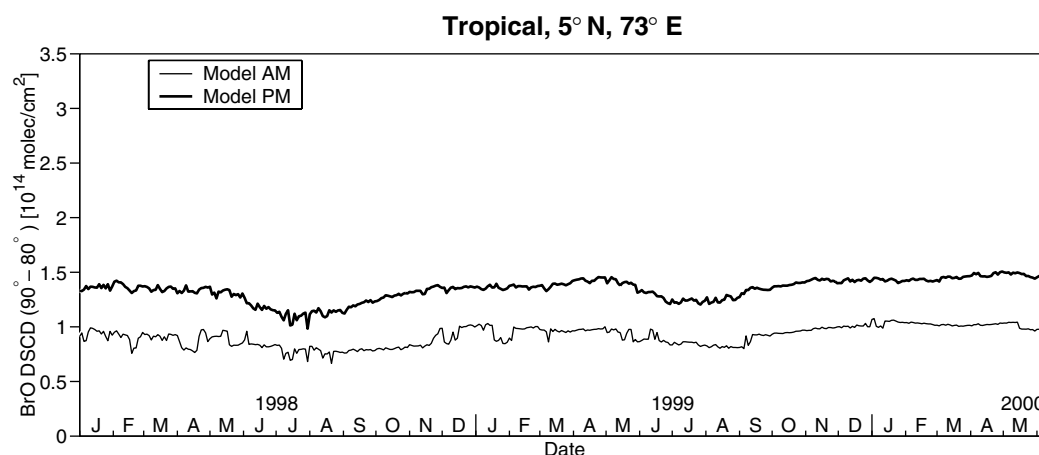
[44] Table 4 summarizes the calculated impact of the uncertainties of reaction rate constants on the BrO DSCD for the most important reactions. These are the formation and the (photolytic) loss reactions for the reservoir species

$BrONO_2$, HOBr and, under situations of high chlorine activation, BrCl. For the gas phase reactions (i.e., $BrO + NO_2$, $BrO + HO_2$, and $BrO + ClO$) the estimated uncertainties given by the JPL 2000 recommendations have been used. The photolytic loss reactions have been changed rather arbitrarily to match the uncertainty of the corresponding gas phase production rates for comparison. They do not necessarily reflect the estimated uncertainties for these reactions. As can be seen, changing the gas phase production rates or changing the photolytic loss rates leads to a different impact on the BrO DSCD, since the bromine partitioning is not in photochemical steady state at sunrise and sunset.

[45] As a rough estimate for the combined uncertainty of the γ value for reaction (4) and of the modeled background aerosol surface area, we have performed a sensitivity calculation where the bromine nitrate hydrolysis has been reduced by 50%.

Figure 6. Comparison of the measured and modeled difference between the evening and morning BrO DSCD for Observatoire de Haute-Provence (OHP, 44°N) and Lauder (45°S). The error bars represent monthly averages and their standard deviation (1σ).
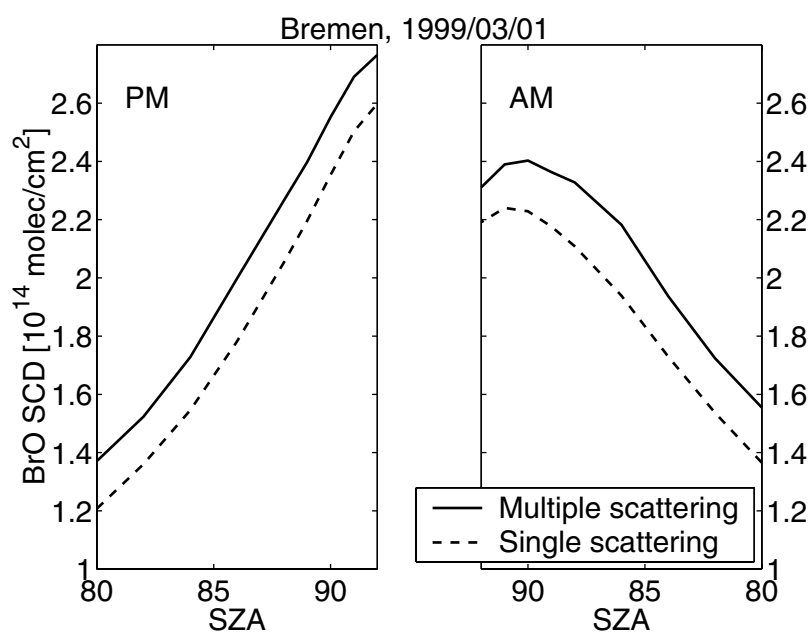
Figure 7. Modeled BrO DSCD for a tropical site (Kaashidhoo, Maldives, 5°N).

[46] Recently *Soller et al.* [2001] found that the reaction of $BrONO_2$ with $O(^3P)$ could be an important loss for bromine nitrate, increasing daytime BrO concentrations. The impact of this reaction on BrO is relatively small in the lower stratosphere, due to the low concentrations of $O(^3P)$, but increases rapidly above about 20 km altitude. We have performed a number of sensitivity calculations were we assume that the products of the reaction $BrONO_2$ + $O(^3P)$ are BrO and NO_3. Including this reaction in the model increases BrO DSCD for typical midlatitude conditions by about 2×10^{13} molecules/cm^2, with larger increases at sunrise than at sunset. Table 4 shows the result for Bremen during March, which is typical for midlatitude situations, with an increase of 21% at sunrise and 13% at sunset. This will lead to a decrease of the PM-AM difference by -0.5×10^{13} molecules/cm^2, corresponding to a decrease of 17%. At high latitudes during periods of
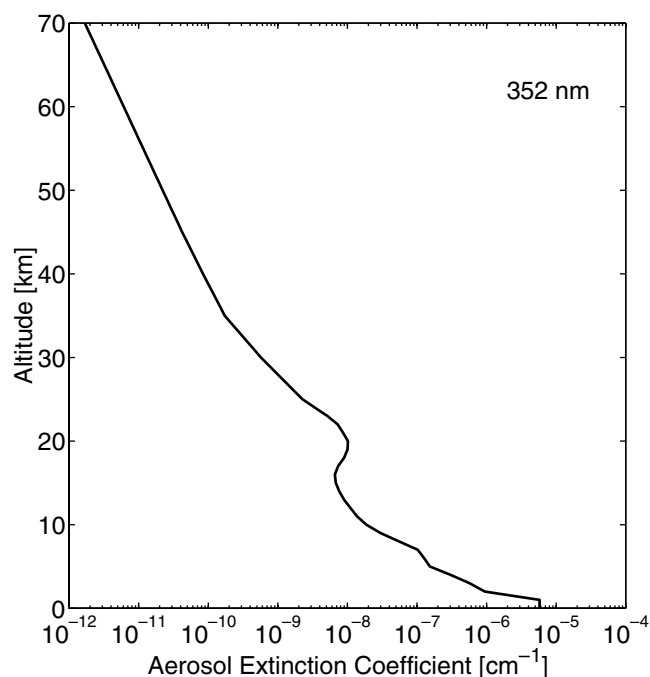
enhanced chlorine activation, however, this reactions has only a minor impact on the BrO DSCD (Table 4).

7. Discussion

[47] As shown in section 5, the model calculation reproduces the observed BrO differential slant columns generally very well. The seasonal and latitudinal variations, as well as the diurnal variations are well captured by the model. For most of the measurement sites observed BrO DSCD are on average 10% higher than the model which assumes a total bromine loading of 20 ppt. This discrepancy could largely be reduced by including the reaction $BrONO_2$ + $O(^3P) \rightarrow$ BrO + NO_3 [*Soller et al.*, 2001]. Taking into account the estimated accuracy of the measurements of about 20% as well as the uncertainties in the model (estimated by the sensitivity studies), the observed BrO DSCD are consistent

Figure 8. The impact of multiple scattering on the calculated BrO slant column.

Figure 9. The aerosol extinction profile assumed for the calculation of the impact of aerosol scattering on BrO slant columns.
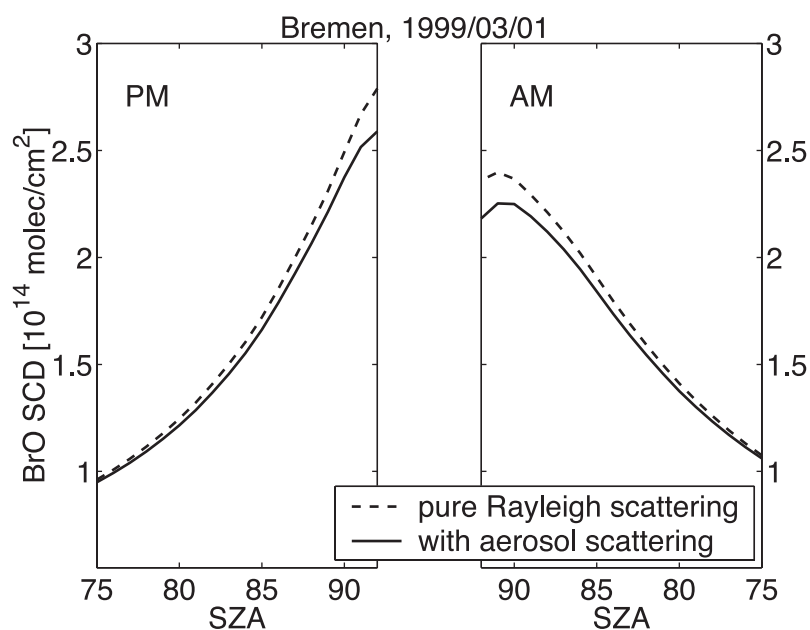
chemistry. The sensitivity studies show that uncertainties in the production rate of $BrONO_2$—either due to uncertainties in the rate constant or due to uncertainties of the NO_2 concentration—will have a large impact on the PM-AM difference of the BrO DSCD. Any changes in the modeled NO_2 concentration alone would thus lead to a discrepancy between observed and modeled PM-AM difference. The situation is different, however, if one takes into account the coupling between individual effects. One of the largest uncertainties for the modeled NO_2 concentrations is the aerosol loading in the model. In fact, there is evidence that for the period considered here the model overestimates the aerosol surface area and thus underestimates the NO_x/NO_y ratio in the lower stratosphere. Reducing the aerosol loading will increase the NO_x/NO_y ratio and will thus decrease BrO by increasing $BrONO_2$. However, the NO_x increase will lead to a HO_x decrease and—even more important here— the decrease of the aerosol loading will reduce the heterogeneous conversion of $BrONO_2$ into HOBr. As a result of these combined effects we find that reducing the aerosol loading in the model reduces the BrO DSCD, but leaves the PM-AM difference largely unchanged.

[49] Including the reaction $BrONO_2 + O(^3P)$ [*Soller et al.*, 2001] decreases the PM-AM difference at midlatitudes by about 0.5 to 1.0×10^{13} molecules/cm^2. This will lead to a better agreement with the Lauder measurements and a slightly worse agreement with the OHP measurements. The main features of the PM-AM differences, however, are not affected by this reaction.

[50] Neglecting the heterogeneous conversion of $BrONO_2$ to HOBr reduces AM BrO DSCD by about 2×10^{13} molecules/cm^2 for typical midlatitude situations, while the PM DSCD are practically unchanged (see also Table 4). The inclusion of the heterogeneous conversion of $BrONO_2$ to HOBr in the model thus clearly results in a better agreement of the modeled BrO AM/PM ratio with obser-

with a stratospheric bromine loading of about 20 ± 4 ppt. This agrees well with the estimated inorganic bromine loading of 21.5 ± 3.0 ppt, as derived for air of 5.6 years mean age for winter 1998/1999 by *Pfeilsticker et al.* [2000].

[48] The good agreement between the observed and modeled AM/PM variation provides strong evidence that the model correctly reproduces the BrO-related bromine
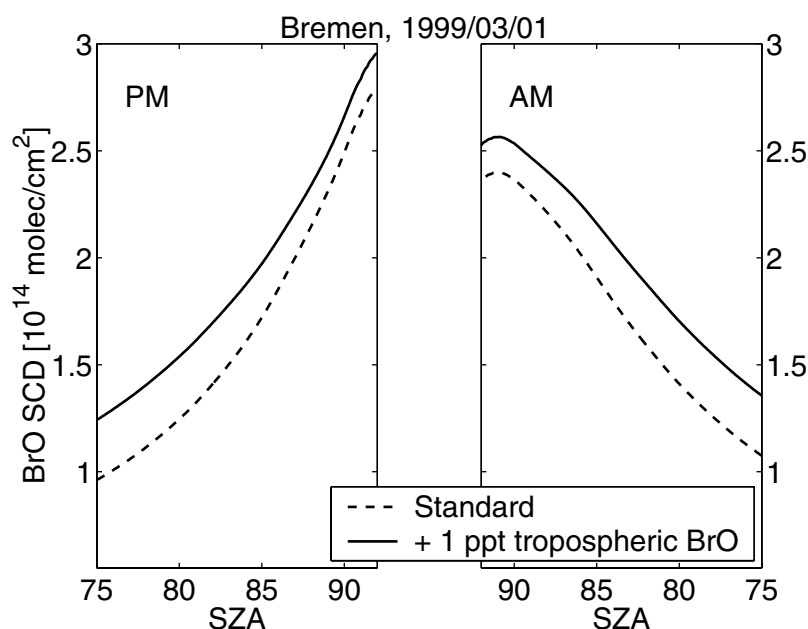

Figure 10. The impact of aerosol scattering on the calculated BrO slant column, based on the assumed aerosol profile shown in Figure 9.

Figure 11. The impact of an assumed tropospheric BrO background on the calculated BrO slant column. The calculations assumed an additional uniform BrO contribution of 1 ppt between the ground and the lowest model level at 330 K.

vations. So although the BrO observations presented here do not prove that HOBr is the major bromine reservoir before sunrise, the good agreement between model and observations for the AM/PM ratio provides strong evidence that HOBr is indeed the major bromine reservoir before sunrise. In addition the rapid increase of HO_x at sunrise, observed during the SPADE campaign [*Salawitch et al.*, 1994] is consistent with the heterogeneous conversion of $BrONO_2$ to HOBr [see also *Lary et al.*, 1996]. It thus seems very unlikely that OBrO is a significant nighttime bromine reservoir, as suggested by *Renard et al.* [1998].

[51] The discrepancy between observed and modeled BrO DSCD at high latitude spring for situations of high chlorine activation can be explained most easily by the given uncertainty of the reaction $BrO + ClO \rightarrow BrCl + O_2$ or the photolysis of BrCl. Increasing the rate constant for the reaction $BrO + ClO \rightarrow BrCl + O_2$ to the upper limit of the JPL 2000 recommendation brings the model in good agreement with the observations during periods of high chlorine activation. For all other situations, and especially high latitude fall, the BrO DSCD remain unaffected by changing this rate constant. As the production of BrCl is the

rate limiting step for one channel of the BrO/ClO ozone loss cycle, increasing the rate constant would have an impact on the calculated ozone loss, both at high and midlatitudes. This would be even more important if also the other

Table 4. Impact of Reaction Rate Uncertainties on the Calculated BrO 90–80° Differential Slant Column Densities[a]

Reaction	Change of Rate Constant, %	Change of BrO DSCD, %		
		AM	PM	PM–AM
Midlatitude				
$BrO + NO_2 + M \rightarrow BrONO_2 + M$	−25[b]	+5	+17	+54
$BrONO_2 + h\nu \rightarrow Br + NO_3$	+25[c]	+7	+9	+13
$BrO + HO_2 \rightarrow HOBr + O_2$	−50[b]	+4	+2	−5
$HOBr + h\nu \rightarrow Br + OH$	+100[c]	+23	+2	−70
$BrONO_2 + H_2O(aq) \rightarrow$ HOBr + HNO_3	−50[d]	−8	−0.5	+26
$BrONO_2 + O(^3P) \rightarrow$ products	included[f]	+21	+13	−17
Polar				
$BrO + ClO \rightarrow BrCl + O_2$	+115[e]	−12	−18	+61
$BrCl + h\nu \rightarrow Br + Cl$	−50[c]	−12	−15	+25
$BrONO_2 + O(^3P) \rightarrow$ products	included[f]	+3	+3	+2

[a] Calculations have been performed for Bremen, 1 March 1999 (midlatitude case, in which very similar results are obtained for different scenarios), and Harestua, 29 January 2000 (polar case).

[b] The change in rate constant refers to a stratospheric temperature of 210 K in the midlatitude case and 193 K in the polar case. They correspond to the estimated uncertainty of the rate constants given by the JPL 2000 recommendations [*Sander et al.*, 2000].

[c] Photolysis rates have been scaled to match the change in the corresponding gas phase reactions for comparison. They do not necessarily reflect estimated uncertainties for these reactions.

[d] The 50% reduction corresponds roughly to the estimated uncertainty in the modeled background aerosol surface area.

[e] The 115% increase corresponds to the difference between the upper limit of the JPL 2000 recommendations and the value of the JPL 1997 recommendations, used for the calculations in Figure 5. The estimated uncertainty for the reaction rate is about ±65% at 193K [*Sander et al.*, 2000].

[f] Reaction rate according to *Soller et al.* [2001]. Here, we assume that the products are $BrO + NO_3$.

Table 3. Impact of Different Processes on the Calculated BrO 90–80° Differential Slant Column Densities[a]

	Change of BrO DSCD, %		
	AM	PM	PM–AM
"Multiple scattering"	−2	+3	+18
"Aerosol"	−9	−7	−2
"tropospheric BrO"	−13	−10	0

"Multiple scattering" is the change between a calculation with multiple scattering and a calculation with single scattering. "Aerosol" is the change between a calculation with additional aerosol scattering and a calculation with Rayleigh scattering only. "Tropospheric BrO" is the change for a calculation with an additional 1 ppt BrO in the troposphere.

[a] Calculations have been performed for Bremen, 1 March 1999.

channels of the BrO + ClO reaction were to be increased, as might be suggested by the fact that laboratory measurements showed a fairly constant branching ratio of about 8% for the BrCl producing channel over a wide range of temperatures [*Atkinson et al.*, 2000, and references therein].

[52] However, there may also be other reasons for the discrepancy between measured and modeled BrO DSCD during late winter and spring at high latitudes, such as events of enhanced tropospheric BrO. Such events can clearly be identified for individual days in the BrO measurements at all polar sites (Ny-Ålesund, Neumayer, and Arrival Heights). Therefore, we may speculate that, in addition, less clearly identifiable events of enhanced tropospheric BrO may lead to a general decrease of the observed BrO DSCD at polar sites during spring.

[53] Recently, *Avallone and Toohey* [2001] suggested that the adduct BrOOCl may form a significant bromine reservoir under cold conditions with high chlorine activation. While this could possibly explain our observed BrO discrepancy qualitatively, a quantitative analysis has to await further studies of the reaction kinetics of the BrOOCl adduct.

8. Conclusions

[54] We have presented ground-based UV–visible measurements of BrO slant column densities from a near-global network. These measurements allow us to draw a picture of the global distribution of stratospheric BrO, especially its seasonal and latitudinal variations. Comparison with calculated BrO slant columns from the SLIMCAT three-dimensional chemical transport model generally show a very good agreement. Moreover, the observational data set itself shows a remarkable internal consistency. In fact, the comparison with the model can help to assess the internal consistency of the BrO time series at one station and the consistency between the BrO measurements at different stations. This study shows that the analysis of the ground-based UV–visible BrO measurements has reached a level where the overall accuracy is to a large extent limited by uncertainties in the BrO absorption cross-section.

[55] The model reproduces the seasonal and latitudinal variations of the BrO DSCD well, indicating that our understanding of the basic features controlling stratospheric BrO is correct. A discrepancy between observed and modeled BrO DSCD of about 10% on average could largely be resolved by including the reaction $BrONO_2 + O(^3P)$ [*Soller et al.*, 2001]. Taking this into account, the observations are consistent with a current stratospheric bromine loading of about 20 ± 4 ppt, in excellent agreement with previous estimates.

[56] In particular the comparison between observed and modeled AM/PM variation of BrO is a critical test for our understanding of stratospheric bromine chemistry. The good agreement provides strong evidence that the model correctly reproduces stratospheric bromine chemistry.

[57] For high latitude spring under situations of chlorine activation, the model overestimates the BrO differential slant column densities. We showed that this discrepancy is within the estimated uncertainty of the rate constant for the reaction $BrO + ClO \rightarrow BrCl + O_2$. Increasing the rate constant to the JPL 2000 upper limit brings the model in

good agreement with the observations. As this would have implications for the calculated ozone loss, it deserves further attention. However, other processes, such as possible tropospheric BrO contributions could in principle also lead to a reduction of the BrO DSCD at high latitudes in spring, and cannot be ruled out at this stage.

[58] The good agreement between the model and the observations gives us confidence that we have correctly identified the relevant mechanisms controlling the global distribution of stratospheric BrO and we can use the model to estimate the impact of bromine on stratospheric ozone depletion.

References

Aliwell, S. R., R. L. Jones, and D. J. Fish, Mid-latitude observations of the seasonal variation of BrO, 1, Zenith-sky measurements, *Geophys. Res. Lett.*, *24*, 1195–1198, 1997.

Aliwell, S. R., et al., Analysis for BrO in zenith-sky spectra: An intercomparison exercise for analysis improvement, *J. Geophys. Res.*, *107*, 10.1029/2001JD000329, 2002.

Arpag, K. H., P. V. Johnston, H. L. Miller, R. W. Sander, and S. Solomon, Observations of stratospheric BrO column over Colorado, 40°N, *J. Geophys. Res.*, *99*, 8175–8181, 1994.

Atkinson, R., D. L. Baulch, R. A. Cox, R. F. Hampson Jr., J. A. Kerr, M. J. Rossi, and J. Troe, Evaluated kinetic and photochemical data for atmospheric chemistry, Supplement VIII, Halogen species, IUPAC subcommittee on gas kinetic data evaluation for atmospheric chemistry, *J. Phys. Chem. Ref. Data*, *29*, 167–266, 2000.

Avallone, L. M., and D. W. Toohey, Tests of halogen photochemistry using in situ measurements of ClO and BrO in the lower stratosphere, *J. Geophys. Res.*, *106*, 10,411–10,421, 2001.

Avallone, L. M., D. W. Toohey, S. M. Schauffler, W. H. Pollock, L. E. Heidt, E. L. Atlas, and K. R. Chan, In situ measurements of BrO during AASE II, *Geophys. Res. Lett.*, *22*, 831–834, 1995.

Bates, D. R., Rayleigh scattering by air, *Planet. Space Sci.*, *32*, 785–790, 1984.

Bekki, S., and J. A. Pyle, A two-dimensional modeling study of the volcanic eruption of Mount Pinatubo, *J. Geophys. Res.*, *99*, 18,861–18,869, 1994.

Brown, S., R. Talukdar, and A. Ravishankara, Rate constants for the reaction $OH + NO_2 + M \rightarrow HNO_3 + M$ under atmospheric conditions, *Chem. Phys. Lett.*, *299*, 277–284, 1999a.

Brown, S., R. Talukdar, and A. Ravishankara, Reconsideration of the rate constant for the reaction of hydroxyl radicals with nitric acid, *J. Phys. Chem. A*, *103*, 3031–3037, 1999b.

Brune, W. H., D. W. Toohey, J. G. Anderson, W. L. Starr, J. F. Vedder, and E. F. Danielsen, In situ northern mid-latitude observations of ClO, O_3, and BrO in the wintertime lower stratosphere, *Science*, *242*, 558–562, 1988.

Brune, W. H., J. G. Anderson, and K. R. Chan, In situ observations of BrO over Antarctica: ER-2 aircraft results from 54°S to 72°S latitude, *J. Geophys. Res.*, *94*, 16,639–16,647, 1989.

Carroll, M. A., R. W. Sanders, S. Solomon, and A. L. Schmeltekopf, Visible and near-ultraviolet spectroscopy at McMurdo station, Antarctica, 6, Observations of BrO, *J. Geophys. Res.*, *94*, 16,633–16,638, 1989.

Chipperfield, M., Multiannual simulations with a three-dimensional chemical transport model, *J. Geophys. Res.*, *104*, 1781–1805, 1999.

Chipperfield, M. P., and J. A. Pyle, Model sensitivity studies of Arctic ozone depletion, *J. Geophys. Res.*, *103*, 28,389–28,403, 1998.

Chipperfield, M. P., D. E. Shallcross, and D. J. Lary, A model study of the potential role of the reaction BrO + OH in the production of stratospheric HBr, *Geophys. Res. Lett.*, *24*, 3025–3028, 1997.

Chipperfield, M. P., T. Glassup, I. Pundt, and O. V. Rattigan, Model calculations of stratospheric OBrO indicating very small abundances, *Geophys. Res. Lett.*, *25*, 3575–3578, 1998.

Daniel, J. S., S. Solomon, R. W. Portmann, and R. R. Garcia, Stratospheric ozone destruction: The importance of bromine relative to chlorine, *J. Geophys. Res.*, *104*, 23,871–23,880, 1999.

DeMore, W. B., S. P. Sander, D. M. Golden, R. F. Hampson, M. J. Kurylo, C. J. Howard, A. R. Ravishankara, C. E. Kolb, and M. J. Molina, Chemical Kinetics and Photochemical Data for Use in Stratospheric Modeling, *JPL Publ. 97-4*, NASA Jet Propul. Lab., 1997.

Dvortsov, V. L., M. A. Geller, S. Solomon, S. M. Schauffler, E. L. Atlas, and D. R. Blake, Rethinking reactive halogen budgets in the midlatitude lower stratosphere, *Geophys. Res. Lett.*, *26*, 1699–1702, 1999.

Eisinger, M., A. Richter, A. Ladstätter-Weißenmayer, and J. P. Burrows, DOAS zenith sky observations, 1, BrO measurements over Bremen (53°N) 1993–1994, *J. Atmos. Chem.*, *26*, 93–108, 1997.

Erle, F., A. Grendel, D. Perner, U. Platt, and K. Pfeilsticker, Evidence of heterogeneous bromine chemistry on cold stratospheric sulphate aerosols, *Geophys. Res. Lett.*, *25*, 4329–4332, 1998.

Erle, F., U. Platt, and K. Pfeilsticker, Measurement of OBrO upper limits in the nighttime stratosphere, *Geophys. Res. Lett.*, *27*, 2217–2220, 2000.

Fish, D. J., R. L. Jones, and E. K. Strong, Midlatitude observations of the diurnal variation of stratospheric BrO, *J. Geophys. Res.*, *100*, 18,863–18,871, 1995.

Fish, D. J., S. R. Aliwell, and R. L. Jones, Mid-latitude observations of the seasonal variation of BrO, 2, Interpretation and modelling study, *Geophys. Res. Lett.*, *24*, 1199–1202, 1997.

Fitzenberger, R., H. Bösch, C. Camy-Peyret, M. P. Chipperfield, H. Harder, U. Platt, B.-M. Sinnhuber, T. Wagner, and K. Pfeilsticker, First profile measurements of tropospheric BrO, *Geophys. Res. Lett.*, *27*, 2921–2924, 2000.

Fraser, P. J., D. E. Oram, C. E. Reeves, S. A. Penkett, and A. McCulloch, Southern hemisphere halon trends (1989–1998) and global halon emissions, *J. Geophys. Res.*, *104*, 15,985–15,999, 1999.

Frieß, U., M. Chipperfield, H. Harder, C. Otten, U. Platt, J. Pyle, T. Wagner, and K. Pfeilsticker, Intercomparison of measured and modeled BrO slant column amounts for the Arctic winter and spring 1994–1995, *Geophys. Res. Lett.*, *26*, 1861–1864, 1999.

Frieß, U., T. Wagner, and U. Platt, Measurement and analysis of tropospheric BrO-events in the Antarctic marine boundary layer, in *Proceedings of the EGS XXVI General Assembly, Nice, France*, p. 1017, 2001.

Hanson, D. R., and A. R. Ravishankara, Heterogeneous chemistry of bromine species in sulfuric acid under stratospheric conditions, *Geophys. Res. Lett.*, *22*, 385–388, 1995.

Hanson, D. R., A. R. Ravishankara, and E. R. Lovejoy, Reaction of $BrONO_2$ with H_2O on submicron sulfuric acid aerosol and the implications for the lower stratosphere, *J. Geophys. Res.*, *101*, 9063–9069, 1996.

Harder, H., et al., Stratospheric BrO profiles measured at different latitudes and seasons: Atmospheric observations, *Geophys. Res. Lett.*, *25*, 3843–3846, 1998.

Harder, H., H. Bösch, C. Camy-Peyret, M. P. Chipperfield, R. Fitzenberger, S. Payan, D. Perner, U. Platt, B.-M. Sinnhuber, and K. Pfeilsticker, Comparison of measured and modeled stratospheric BrO: Implications for the total amount of stratospheric bromine, *Geophys. Res. Lett.*, *27*, 3695–3698, 2000.

Harwood, M. H., J. B. Burkholder, and A. R. Ravishankara, Photodissociation of $BrONO_2$ and N_2O_5: Quantum yields for NO_3 production at 248, 308, and 352.5 nm, *J. Phys. Chem.*, *102*, 1309–1317, 1998.

Hendrick, F., et al., Simulation of BrO diurnal variation and BrO slant columns: Intercomparison exercise between three model packages, in *Proceedings of the Fifth European Symposium on Stratospheric Ozone*, Eur. Comm. Air Pollut. Res. Rep. 73, pp. 256–259, 1999.

Ingham, T., D. Bauer, J. Landgraf, and J. N. Crowley, Ultraviolet–visible absorption cross sections of gaseous HOBr, *J. Phys. Chem. A*, *102*, 3293–3298, 1998.

Johnson, D. G., W. A. Traub, K. V. Chance, and K. W. Jucks, Detection of HBr and upper limit for HOBr: Bromine partitioning in the stratosphere, *Geophys. Res. Lett.*, *22*, 1373–1376, 1995.

Ko, M. K. W., N.-D. Sze, C. J. Scott, and D. K. Weisenstein, On the relation between stratospheric chlorine/bromine loading and short-lived tropospheric source gases, *J. Geophys. Res.*, *102*, 25,507–25,517, 1997.

Kreher, K., P. V. Johnston, S. W. Wood, B. Nardi, and U. Platt, Ground-based measurements of tropospheric and stratospheric BrO at Arrival Heights, Antarctica, *Geophys. Res. Lett.*, *24*, 3021–3024, 1997.

Lary, D. J., Gas phase atmospheric bromine photochemistry, *J. Geophys. Res.*, *101*, 1505–1516, 1996.

Lary, D. J., M. P. Chipperfield, R. Toumi, and T. Lenton, Heterogeneous atmospheric bromine chemistry, *J. Geophys. Res.*, *101*, 1489–1504, 1996.

Liou, K. N., *Radiation and Cloud Processes in the Atmosphere*, 487 pp., Oxford Univ. Press, New York, 1992.

McKinney, K. A., J. M. Pierson, and D. W. Toohey, A wintertime in situ profile of BrO between 17 and 27 km in the Arctic vortex, *Geophys. Res. Lett.*, *24*, 853–856, 1997.

Müller, R. W., H. Bovensmann, J. W. Kaiser, A. Richter, A. Rozanov, F. Wittrock, and J. P. Burrows, Consistent interpretation of ground based and GOME BrO slant column data, *Adv. Space Res.*, *29*, 1655–1660, 2002.

Otten, C., F. Ferlemann, U. Platt, T. Wagner, and K. Pfeilsticker, Ground-based DOAS UV/visible measurements at Kiruna (Sweden) during SESAME winters 1993/94 and 1994/95, *J. Atmos. Chem.*, *30*, 141–162, 1998.

Pfeilsticker, K., W. T. Sturges, H. Bösch, C. Camy-Peyret, M. P. Chipperfield, A. Engel, R. Fitzenberger, M. Müller, S. Payan, and B.-M. Sinnhuber, Lower stratospheric organic and inorganic bromine budget for the Arctic winter 1998/99, *Geophys. Res. Lett.*, *27*, 3305–3308, 2000.

Platt, U., Differential optical absorption spectroscopy (DOAS), in *Air Monitoring by Spectroscopic Techniques*, Chem. Anal. Ser., vol. 127, edited by M. W. Sigrist, pp. 27–84, John Wiley, New York, 1994.

Pundt, I., et al., Simultaneous UV–vis measurements of BrO from balloon, satellite and ground: Implications for tropospheric BrO, in *Proceedings of the Fifth European Symposium on Stratospheric Ozone*, Eur. Comm. Air Pollut. Res. Rep. 73, pp. 316–319, 1999a.

Pundt, I., J. P. Pommereau, F. Goutail, M. P. Chipperfield, F. Danis, N. R. P. Harris, and J. A. Pyle, Vertical distribution of BrO and Bry at high, mid-, and low latitudes, in *Proceedings of the Fifth European Symposium on Stratospheric Ozone*, Eur. Comm. Air Pollut. Res. Rep. 73, pp. 312–315, 1999b.

Renard, J. B., M. Pirre, C. Robert, and D. Huguenin, The possible detection of OBrO in the stratosphere, *J. Geophys. Res.*, *103*, 25,383–25,395, 1998.

Richter, A., F. Wittrock, M. Eisinger, and J. P. Burrows, GOME observations of tropospheric BrO in northern hemispheric spring and summer 1997, *Geophys. Res. Lett.*, *25*, 2683–2686, 1998.

Richter, A., M. Eisinger, A. Ladstätter-Weißenmayer, and J. P. Burrows, DOAS zenith sky observations, 2, Seasonal variation of BrO over Bremen (53°) 1994–1995, *J. Atmos. Chem.*, *32*, 83–99, 1999.

Rozanov, A., V. Rozanov, and J. P. Burrows, A numerical radiative transfer model for a spherical planetary atmosphere: Combined differential–integral approach involving the Picard iterative approximation, *J. Quant. Spectrosc. Radiat. Transfer*, *69*, 491–512, 2001.

Salawitch, R. J., et al., The diurnal variation of hydrogen, nitrogen, and chlorine radicals: Implications for the heterogeneous production of HNO_2, *Geophys. Res. Lett.*, *21*, 2551–2554, 1994.

Sander, S. P., et al., Chemical Kinetics and Photochemical Data for Use in Stratospheric Modeling, *JPL Publ. 00-3*, NASA Jet Propul. Lab., 2000.

Sarkissian, A., H. K. Roscoe, and D. J. Fish, Ozone measurements by zenith-sky spectrometers: An evaluation of errors in air-mass factors calculated by radiative transfer models, *J. Quant. Spectrosc. Radiat. Transfer*, *54*, 471–480, 1995.

Schauffler, S. M., E. L. Atlas, D. R. Blake, F. Flocke, R. A. Lueb, J. M. Lee-Taylor, V. Stroud, and W. Travnicek, Distributions of brominated organic compounds in the troposphere and lower stratosphere, *J. Geophys. Res.*, *104*, 21,513–21,535, 1999.

Slusser, J. R., D. J. Fish, E. K. Strong, R. L. Jones, H. K. Roscoe, and A. Sarkissian, Five years of NO_2 vertical column measurements at Faraday (65°S): Evidence for the hydrolysis of $BrONO_2$ on Pinatubo aerosols, *J. Geophys. Res.*, *102*, 12,987–12,993, 1997.

Soller, R., J. M. Nicovich, and P. H. Wine, Temperature-dependent rate coefficients for the reactions of $Br(^2P_{3/2})$, $Cl(^2P_{3/2})$, and $O(^3PJ)$ with $BrONO_2$, *J. Phys. Chem. A*, *105*, 1416–1422, 2001.

Solomon, S., A. L. Schmeltekopf, and R. W. Sanders, On the interpretation of zenith sky absorption-measurements, *J. Geophys. Res.*, *92*, 8311–8319, 1987.

South, A. M., N. Mohamed-Tahrin, R. A. Freshwater, and R. L. Jones, Ground-based observations of BrO over Huelva, Spain (37°N), in *Proceedings of the Fifth European Symposium on Stratospheric Ozone*, Eur. Comm. Air Pollut. Res. Rep. 73, pp. 356–359, 1999.

Sturges, W. T., D. E. Oram, L. J. Carpenter, S. A. Penkett, and A. Engel, Bromoform as a source of stratospheric bromine, *Geophys. Res. Lett.*, *27*, 2081–2084, 2000.

Sturges, W. T., H. P. McIntyre, S. A. Penkett, J. Chappellaz, M. J.-Barnola, R. Mulvaney, E. Atlas, and V. Stroud, Methyl bromide, other brominated methanes, and methyl iodide in polar firn air, *J. Geophys. Res.*, *106*, 1595–1606, 2001.

Swinbank, R., and A. O'Neill, A stratosphere–troposphere data assimilation system, *Mon. Weather Rev.*, *122*, 686–702, 1994.

Toohey, D. W., J. G. Anderson, W. H. Brune, and K. R. Chan, In situ measurements of BrO in the Arctic stratosphere, *Geophys. Res. Lett.*, *17*, 513–516, 1990.

Tørnkvist, K. K., D. W. Arlander, and B.-M. Sinnhuber, Ground-based UV measurements of BrO and OClO over Ny-Ålesund during Winter

1996 and 1997 and Andøya (1998/99), *J. Atmos. Chem.*, *43*, 75–106, 2002.

Van Roozendael, M., C. Fayt, F. Hendrick, C. Hermans, J.-C. Lambert, D. Forteyn, B.-M. Sinnhuber, and M. P. Chipperfield, Seasonal and diurnal variations of BrO column abundances above Harestua (60°N) and Haute-Provence (44°N) during THESEO, in *Proceedings of the Fifth European Symposium on Stratospheric Ozone*, Eur. Comm. Air Pollut. Res. Rep. 73, pp. 332–335, 1999a.

Van Roozendael, M., C. Fayt, J.-C. Lambert, I. Pundt, T. Wagner, A. Richter, and K. Chance, Development of a bromine oxide product from GOME, in *Proceedings of the European Symposium on Atmospheric Measurements from Space (ESAMS 99)*, 18–22 January, ESTEC, Noordwijk, Netherlands, WPP-161, pp. 543–547, Eur. Space Agency, Noordwijk, Netherlands, 1999b.

Wagner, T., and U. Platt, Satellite mapping of enhanced BrO concentrations in the troposphere, *Nature*, *395*, 486–490, 1998.

Wagner, T., C. Leue, M. Wenig, K. Pfeilsticker, and U. Platt, Spatial and temporal distribution of enhanced boundary layer BrO concentrations measured by the GOME instrument aboard ERS-2, *J. Geophys. Res.*, *106*, 24,225–24,236, 2001.

Wamsley, P. R., et al., Distribution of halon-1211 in the upper troposphere and lower stratosphere and the 1994 total bromine budget, *J. Geophys. Res.*, *103*, 1513–1526, 1998.

Wennberg, P. O., et al., Removal of stratospheric O_3 by radicals: In situ measurements of OH, HO_2, NO, NO_2, ClO, and BrO, *Science*, *266*, 398–404, 1994.

World Meteorological Organization (WMO), Scientific Assessment of Ozone Depletion: 1998, Global Ozone Research and Monitoring Project, Rep. No. 44, 1999.

───────────

D. W. Arlander and K. K. Tørnkvist, Norwegian Institute for Air Research, Kjeller, Norway.

H. Bovensmann, J. P. Burrows, R. Müller, A. Richter, B.-M. Sinnhuber, and F. Wittrock, Institute of Environmental Physics, University of Bremen, Germany. (bms@iup.physik.uni-bremen.de)

M. P. Chipperfield, School of the Environment, University of Leeds, Leeds, LS2 9JT, UK.

C.-F. Enell, Swedish Institute of Space Physics, Kiruna, Sweden.

U. Frieß, K. Pfeilsticker, U. Platt, and T. Wagner, Institute of Environmental Physics, University of Heidelberg, Germany.

F. Hendrick and M. Van Roozendael, Belgian Institute for Space Aeronomy, Brussels, Belgium.

P. V. Johnston and K. Kreher, National Institute of Water and Atmospheric Research, Lauder, New Zealand.

R. L. Jones, N. Mohamed-Tahrin, and A. M. South, Center for Atmospheric Science, University of Cambridge, UK.

J.-P. Pommereau and I. Pundt, Service d'Aéronomie, Verrières-le-Buisson, France.